



Implantable and Biodegradable Macroporous Iron Oxide Frameworks for Efficient Regeneration and Repair of Infarcted Heart

Citation

Wang, W., H. Tao, Y. Zhao, X. Sun, J. Tang, C. Selomulya, J. Tang, et al. 2017. "Implantable and Biodegradable Macroporous Iron Oxide Frameworks for Efficient Regeneration and Repair of Infarcted Heart." *Theranostics* 7 (7): 1966-1975. doi:10.7150/thno.16866. <http://dx.doi.org/10.7150/thno.16866>.

Published Version

doi:10.7150/thno.16866

Permanent link

<http://nrs.harvard.edu/urn-3:HUL.InstRepos:33490803>

Terms of Use

This article was downloaded from Harvard University's DASH repository, and is made available under the terms and conditions applicable to Other Posted Material, as set forth at <http://nrs.harvard.edu/urn-3:HUL.InstRepos:dash.current.terms-of-use#LAA>

Share Your Story

The Harvard community has made this article openly available.
Please share how this access benefits you. [Submit a story](#).

[Accessibility](#)

Research Paper

Implantable and Biodegradable Macroporous Iron Oxide Frameworks for Efficient Regeneration and Repair of Infarcted Heart

Wenshuo Wang^{1*}, Hongyue Tao^{4*}, Yun Zhao¹, Xiaotian Sun^{5*}, Jing Tang², Cordelia Selomulya³, Jia Tang⁶, Tianchan Chen⁶, Yang Wang³, Minglei Shu⁶, Lei Wei⁶, Guanyu Yi⁶, Jixue Zhou⁶, Lai Wei¹✉, Chunsheng Wang¹, and Biao Kong⁷✉

1. Department of Cardiac Surgery, Zhongshan Hospital, Fudan University, Shanghai 200032, P. R. China

2. Department of Anesthesiology, Division of Critical Care Medicine, Boston Children's Hospital, Harvard Medical School, 300 Longwood Avenue, Boston, Massachusetts 02115, USA

3. Department of Chemical Engineering, Monash University, Clayton, Victoria 3800, Australia

4. Department of Radiology, Huashan Hospital, Fudan University, Shanghai 200040, P. R. China

5. Department of Cardiothoracic Surgery, Huashan Hospital, Fudan University, Shanghai 200040, P. R. China

6. National Supercomputer Research Center of Advanced Materials, Shandong Key Laboratory for High Strength Lightweight Metallic Materials, Advanced Materials Institute, Shandong Academy of Sciences, Jinan 250014, P. R. China

7. Department of Chemistry, Laboratory of Advanced Materials, Fudan University, Shanghai 200433, P. R. China

* These authors contributed equally to this study

✉ Corresponding authors: Biao Kong (B.K.); Lai Wei (L.W.) Email addresses: bkong@fudan.edu.cn (B.K.); wei.lai@zs-hospital.sh.cn (L.W.)

© Ivyspring International Publisher. This is an open access article distributed under the terms of the Creative Commons Attribution (CC BY-NC) license (<https://creativecommons.org/licenses/by-nc/4.0/>). See <http://ivyspring.com/terms> for full terms and conditions.

Received: 2016.07.16; Accepted: 2016.10.17; Published: 2017.05.02

Abstract

The construction, characterization and surgical application of a multilayered iron oxide-based macroporous composite framework were reported in this study. The framework consisted of a highly porous iron oxide core, a gelatin-based hydrogel intermediary layer and a matrigel outer cover, which conferred a multitude of desirable properties including excellent biocompatibility, improved mechanical strength and controlled biodegradability. The large pore sizes and high extent of pore interconnectivity of the framework stimulated robust neovascularization and resulted in substantially better cell viability and proliferation as a result of improved transport efficiency for oxygen and nutrients. In addition, rat models with myocardial infarction showed sustained heart tissue regeneration over the infarct region and significant improvement of cardiac functions following the surgical implantation of the framework. These results demonstrated that the current framework might hold great potential for cardiac repair in patients with myocardial infarction.

Key words: macroporous frameworks; vasculature; stem cell; blood iron pool; cardiac repair.

Introduction

The advancement in material sciences, synthetic chemistry and nanotechnology has led to an explosion in the variety of frameworks available for tissue grafting [1]. Regardless of components used and structures adopted, the suitability of any implantable framework should always be assessed using the following set of criteria. The foremost requirement is that the framework must offer excellent

biocompatibility, which is vital for effective cell adherence and prolonged cell viability [1]. Ideally, the micro-environment inside the framework should closely resemble the native extracellular matrix (ECM) of the cells and tissues to be grafted. Controlled biodegradability plays an equally important role in the selection and design of framework materials. The degradation of the framework should occur in such a

time frame that ensures sufficient expansion of the grafted tissue, and generate only non-toxic products that can be easily metabolized.

Porous framework-based delivery of stem cells is an emerging treatment approach for patients with myocardial infarction (MI). The blockage of coronary arteries eventually results in irreversible necrosis of the affected heart tissues and severely impaired heart functions [1]. In the past decades, however, the direct injection of neonatal rat cardiomyocytes followed by rapid cell death during the first week leads to the approximate loss of 90% of the total cell population introduced [2]. Furthermore, these unattached cell grafts are also at the risk of being washed away due to the high compressive forces present in the cardiac chambers [2].

Compared to the methods that attempt to directly inject a suspension of stem cells or cardiomyocytes to the infarct zone, the primary advantage of using of an implantable framework is its ability to mimic the architecture of the extracellular matrix. The ECM is generally considered to be essential for cell differentiation and proliferation. Therefore, by being adhered to and insulated by the porous framework would allow stem cells and cardiomyocytes to be physically sequestered at the target area and maximize their chances of retention. Past studies have also suggested the benefit of inducing a mild inflammatory response in the course of framework degradation to stimulate cell proliferation [3, 4]. Another determinant in framework fabrication is the creation of a highly porous, interconnected architecture that allows efficient diffusion of nutrients and metabolic wastes. The pore size of the framework is particularly crucial for cardiac tissue engineering due to a high demand of vascularization [5]. A delicate balance should be maintained between promoting unrestricted cell migration and avoiding excessive internal space that would slow down microvasculature formation [6].

The development of novel implantable frameworks should meet all requirements mentioned above. It is inevitable that many frameworks fare well in some metrics and underperform in others. For example, frameworks comprising naturally occurring polymers, such as collagen [7, 8], gelatin [9], chitosan [10] and other types of polysaccharides and polypeptides [11], are generally quite biocompatible and biodegradable. However, they still suffer significant drawbacks that include poor mechanical integrity, potential immunogenicity, and a lack of tailoring techniques [12]. The alternative is a host of synthetic polymers poly(glycerol sebacate) (PGS) [13], poly(lactide-co-glycolide) (PLGA) [14], poly(ethylene glycol) (PEG) [15, 16], or others [17]. Synthetic

frameworks are generally less susceptible to fracture, offer more customizability, and often elicit a lower level of undesirable immune response from the host. However due to their artificial nature, they often underperform their natural counterparts in serving as a suitable anchorage for cell attachment and growth. Research efforts have thus been increasingly focused on generating composite frameworks to combine the strengths of natural and synthetic materials. Fibrous frameworks consisting of poly(lactic-co-glycolic acid) (PLGA), gelatin and α -elastin were found to induce better three-dimensional (3D) tissue assembly and cell ingrowth with improved mechanical strength [18]. More recently, carbon nanofibers were incorporated into a chitosan-based framework, leading to better conductivity and simultaneous increase in graft viability [19]. Despite these advances, it is often technologically challenging to create frameworks that excel in all desirable metrics, including satisfactory biocompatibility, porosity, malleability, and so on. More importantly, to the best of our knowledge, there has been no concrete experimental data that directly evaluate the surgical benefits of tissue engineering frameworks. The lack of clinical consideration in these studies often leads to the development of tissue engineering frameworks that demonstrate laboratory-proven success but eventually fail to exhibit efficacy in real surgical applications.

In the past several years, we have focused on the development of macroporous materials that exhibited the potential of application in the field of tissue engineering [20, 21, 22]. Especially, we find the way to construct frameworks based on composite materials, which paves the way for satisfying biomedical needs [23]. Herein, we report a multi-layered iron oxide framework that contains a gelatin-based hydrogel intermediary layer and a matrigel outer cover (**Figure 1**). Combining the respective strengths of the individual materials, the framework possesses a hierarchical porous structure that promotes robust 3D cell proliferation and vascularization, and exhibits excellent biocompatibility allowing facile cell adhesion. More importantly, the composite framework also showed a high efficiency in regenerating heart tissues *in vivo* and restoring lost cardiac functions for rats with myocardial infarction (increased $\sim 63\%$ of stroke volume, $\sim 32\%$ of ejection fraction, $\sim 49\%$ of fraction shortening). The composite framework constructed in current study combined the advantages of natural and synthetic materials and owned the potential to release iron ion which may be beneficial in curing myocardial infarction. We envision that this study could pave the way for new development in porous material-based heart tissue engineering frameworks in future.

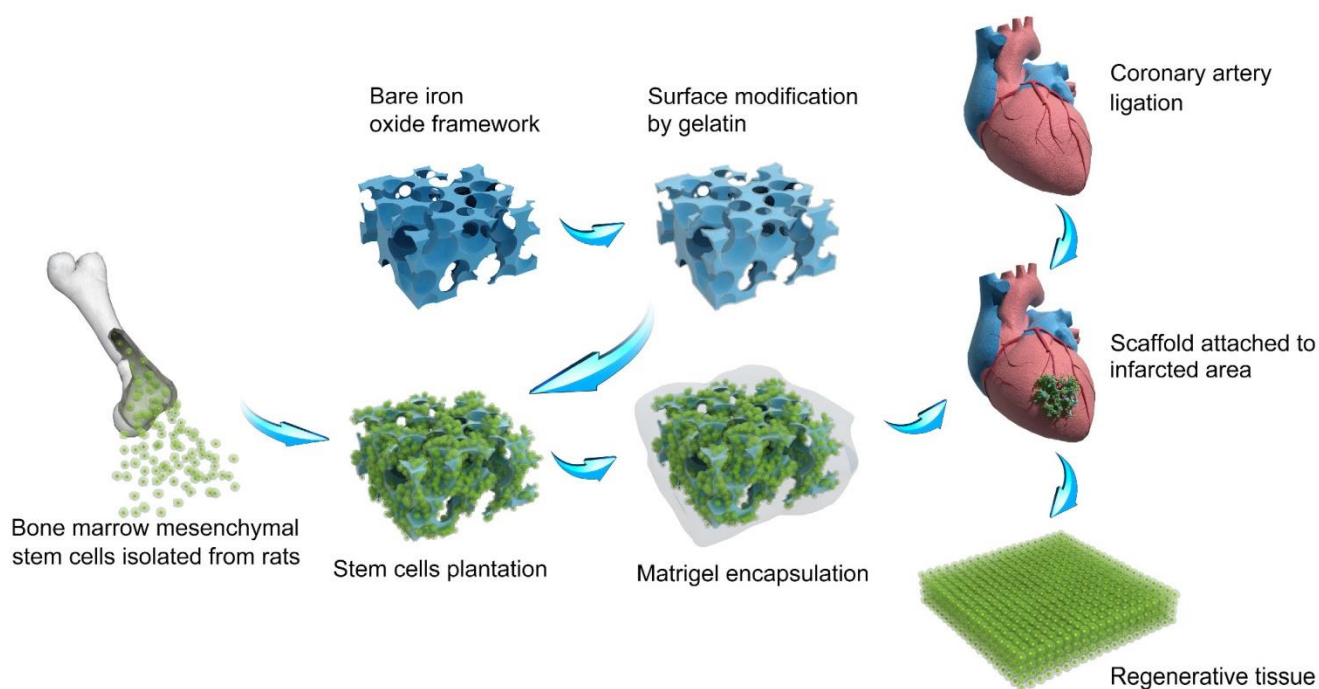


Figure 1. Schematic of the construction of macroporous iron oxide frameworks for efficient regeneration and repair of infarcted heart.

Materials and Methods

The synthesis of macroporous iron oxide frameworks

The construction of an ultralight magnetic framework was obtained by controlled hydrolysis of $K_4[Fe(CN)_6]$ over a polyurethane (PU) sponge to form prussian blue nanocubes, followed by atmospheric pyrolysis that formed macroporous iron oxide structures [24]. Polyurethane (PU) sponges with various pore sizes per linear inch (PPI) were used as a macroporous scaffold for 3D growth of PB. In a typical procedure, 127 mg (0.3 mmol) $K_4Fe(CN)_6 \cdot 3H_2O$ was added to a 80 mL solution of 0.05 M hydrochloric acid (HCl) and stirred for 60 min, followed by the slow, controlled immersion of a 30 cm³ PU sponge. The resulting mixture was heated to 85 °C and maintained at this temperature for 48 h. The framework, then coated with Prussian blue, was dried in a vacuum oven at 40 °C for 12 h and then subjected to pyrolysis at (350, 400, and 450 °C) with a temperate ramp of 1 °C min⁻¹ for 3 h. To remove the remnants $K_4Fe(CN)_6 \cdot 3H_2O$, Prussian blue and PU, as well as various by-products generated in the fabrication process, the iron oxide framework was dialyzed in 10 mL DMSO for 7 days and then in sterile ultrapure water for an additional 7 days. During dialysis, the dialysis buffer was changed every 24 h. The treated framework was then immersed for 2 h in a 2 mL sterile solution of 2% gelatin, which was briefly

sonicated to remove all the air bubbles. The gelatin-coated framework was subsequently allowed to dry in a sterilized ventilation hood.

Cell Seeding

Bone-marrow-derived rat mesenchymal stem cells were isolated from rat shin bones and transfected with an eGFP-carrying lentiviral vector. The transfected cells were seeded on the gelatin-layered framework at a concentration of 3×10^7 per mL, with a total volume of 0.5 mL of cell suspension used. The seeded framework was placed in a clean, sterile petri dish and was incubated at 37 °C for 6 h to allow cell attachment, after which the framework was rinsed 3 times with a combined volume of 15 mL of Dulbecco's Modified Eagle's medium (DMEM), supplemented with 10% fetal bovine serum (FBS), 1% Penicillin-Streptomycin, in order to remove unattached cells. The framework was next placed in 3 mL of fresh DMEM medium supplemented with 10% FBS and 1% Penicillin-Streptomycin and cultivated at 37 °C and under 5% CO₂ over a period of 7 days, during which period the abovementioned medium was changed on a daily basis.

Structural Characterization

The field emission scanning electron microscopy (FESEM) images were carried out on a FE-SEM S-4800 scanning electron microscope (Hitachi, Japan). Confocal fluorescent microscopy images were acquired using a Leica Confocal 1P/FCS microscope.

Matrigel Coating

Once imaging experiments had confirmed the extensive proliferation of the seeded cells, the framework was carefully placed within a clone ring on a clean, sterile petri dish. The clone ring was filled with 200 μ L pre-chilled 10% matrigel solution, allowed to stand for 15 sec and then drained of the solution with the help of a pipette tip. This procedure was subsequently repeated for 20%, 40%, 80% and 100% matrigel solutions. After the addition of the 100% matrigel solution, the clone ring was incubated at 37 °C for 2 h to allow the matrigel to solidify and form the outer layer of the composite framework.

Framework Implantation

Surgical implantation of the iron-oxide-based composite framework onto the heart of healthy rats was performed based on a previously described protocol with minor modifications. The rat was anesthetized with 2% isoflurane using an induction chamber and placed in a supine position. A midline cervical incision was performed to separate the skin, muscle and tissue that covered the trachea. After the exposure of the trachea, a small hole was created into the tissue between two cartridge rings below the glottis to insert the endotracheal tube with micro surgical forceps. Once the lungs were verified to be well ventilated with a respiration rate (RR) of around 110 per minute and an inspiratory pressure of 17-18 cm H₂O, the mouse was repositioned to allow it to lie on its right side and face left. A left-sided thoracotomy was performed between the 3rd and the 4th rib. Once the thorax was opened, the part of the pericardial sac covering the heart was carefully removed without scratching and damaging the lungs, after which the framework was gently attached to the apex of the heart through the application of fibrin sealant (RAAS, Shanghai, China). Subsequently, a chest tube (28G, venal catheter) was placed between the 4th and the 5th rib and the thoracic incision was closed, using 6-0 Prolene running sutures (Ethicon, Norderstedt, Germany) to adapt the ribs and 4-0 Prolene running sutures (Ethicon, Norderstedt, Germany) to close the skin. Once complete, the thorax was drained with a 2 mL syringe and the rat was placed on its back again to facilitate the removal of the endotracheal tube from the trachea, followed by adaptation of the tracheal cartridge rings in one single stitch using 7-0 Prolene sutures (Ethicon, Norderstedt, Germany). Finally, the skin was closed using 4-0 Prolene running sutures (Ethicon, Norderstedt, Germany).

Myocardial Infarction Model

For inducing MI in rats, the identical surgical procedures as implantation surgery were followed,

except that once the pericardial sac covering the rat heart was removed, the left anterior descending artery (LAD), located between the pulmonary artery and the left auricle, was identified and its proximal segment was ligated with one single suture. The treated rats received cell-seeded frameworks as the implantation surgery described and the control rats received sham operation.

Echocardiography

Rats were anesthetized by inhaled isoflurane (1%, Baxter) in normal air. Each animal was fastened to a heating pad and subject to a chemical hair remover (VEET, China) to shave the chest. Pre-warmed ultrasound gel (Hankang, China) was utilized to the thoracic wall to facilitate the visibility of the heart chambers. Echocardiography (M-model and two-dimensional) was performed by a Vevo 2100 high resolution ultrasound machine.

Statistical analysis

All data are derived from the mean of duplicate samples from three independently performed experiments and expressed in the format of mean \pm SEM. Statistical analysis was performed using SPSS (Version 20.0; IBM Corporation, Armonk, NY, USA) via either analysis of variance or Student-Newmann-Keuls multiple comparison test. Differences were considered statistically significant at $P < 0.05$.

Results

The characterization of macroporous iron oxide frameworks

As illustrated in **Figure 2**, the clean, sterile iron oxide framework was visualized to possess an interconnected porous structure. However, the pristine porous iron oxide framework showed poor biocompatibility with mesenchymal stem cells in subsequent cell adhesion assays (data not shown). As evidenced by the scanning electron microscope (SEM), the gelatin-based hydrogel layer significantly smoothed the surface of the iron oxide core, and improved the cell adhesion efficiency.

Macroporous iron oxide frameworks support cellular proliferation and migration

The number of viable cells was monitored by measuring the fluorescence generated by lentivirus-promoted enhanced green fluorescent protein gene transduction. Imaging of the porous framework at 24 h after seeding revealed sporadic fluorescence over its outer surface and further indicated successful cell adhesion (**Figure 3a**). At Day 3, fluorescent cells were observed to have grown extensively along the trabeculae and also started to

penetrate into the pores on the framework (Figure 3b). At Day 7, the proliferated cells had both completely covered the outer surface of the framework and filled up its porous core (Figure 3c). The formation of an extensive 3D cell network was further confirmed by confocal microscopy and 3D image reconstruction (Figure 3d, e). In addition, the cross-section of the framework was visualized by SEM images, which provided unambiguous evidence of cell growth at a depth of 1.5 mm to the surface (Figure 3f). SEM images of a single pore and its surroundings revealed entanglement of thick cell sheets around the frame of the pore (Figure 3g). It is especially noteworthy that the large and highly interconnected pores of the framework allowed the existence of microchannels, which could ensure unfettered nutrient transfer and vascularization, even after the cells had completely enveloped the trabeculae (Figure 3g). Taken together, these imaging results indicated the ability of the framework to promote rapid *in vitro* regeneration of myocardial cells and vasculature.

Matrigel coating increases the compatibility with surgery

Frameworks loaded with stem cells are vulnerable to the procedures of surgery, which may be similar with the failure of vein graft caused by injury during surgery [25]. Depending on the specific circumstances, this could be attributed to the physical damage of the cells during surgical handling, dehydration due to prolonged exposure to air, and so on. In many cases, an additional protective layer is warranted outside the regenerated cells to shield them

from these detrimental factors. After allowing seeded stem cells to grow for 3 days, the framework was coated with a homogenous layer of the matrigel. As illustrated in Figure 4, the matrigel cover did not diminish the fluorescence level of the cells on the framework, indicating that they remained metabolically robust.

Cell-seeded macroporous iron oxide frameworks mitigate the ischemia-induced heart dysfunction

The composite porous framework was subsequently implanted into healthy rats to ascertain whether the regenerated myocardial cells and blood vessels could continue to grow and form functionally competent tissue network *in vivo*. The structural integrity of the implanted framework was first monitored via magnetic resonance imaging (MRI). Immediately following the implantation, the presence of the framework was shown to lead to a decline of T2 signal at the target zone (Figure 5a). After 2 months, subsequent MRI imaging revealed near-complete shrinkage of the low-T2 area around the same zone (Figure 5b), implying that the framework had been largely absorbed. Close examination of the area where the framework was implanted under a stereo fluorescent microscope found a significantly higher level of fluorescence intensity (Figure 5c) compared to the background of nonspecific fluorescence emanated by the framework-free control (Figure 5d), suggesting a sustained growth of the grafted tissues on the heart's surface (the relevant histological result was shown as Supplement Figure 1).

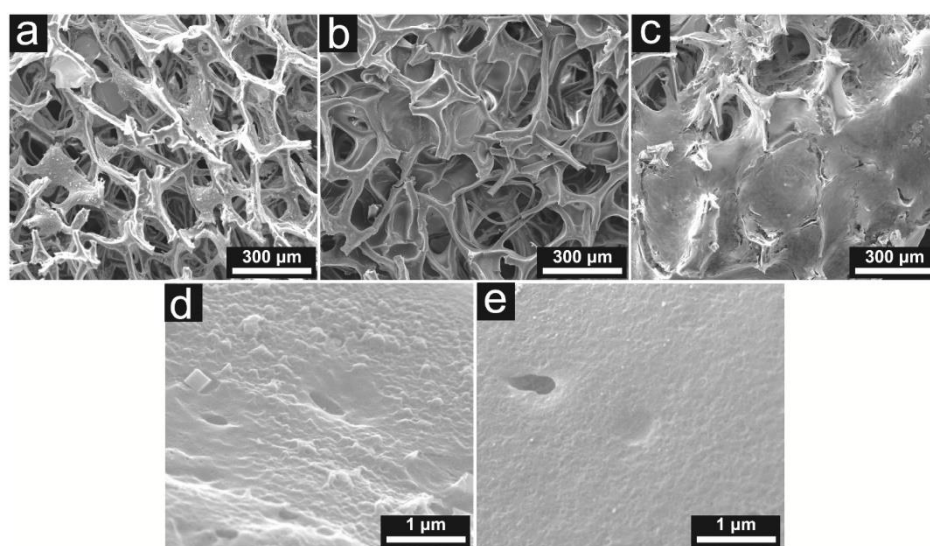


Figure 2. SEM images showing the naked iron oxide framework (a), the gelatin-coated framework (b), and stem cells adhering to and proliferating around the framework trabeculae (c); demonstrating the surface features of the naked iron oxide framework (d) and the gelatin-coated framework (e). It can be seen that the gelatin layer significantly smoothened the surface of the framework.

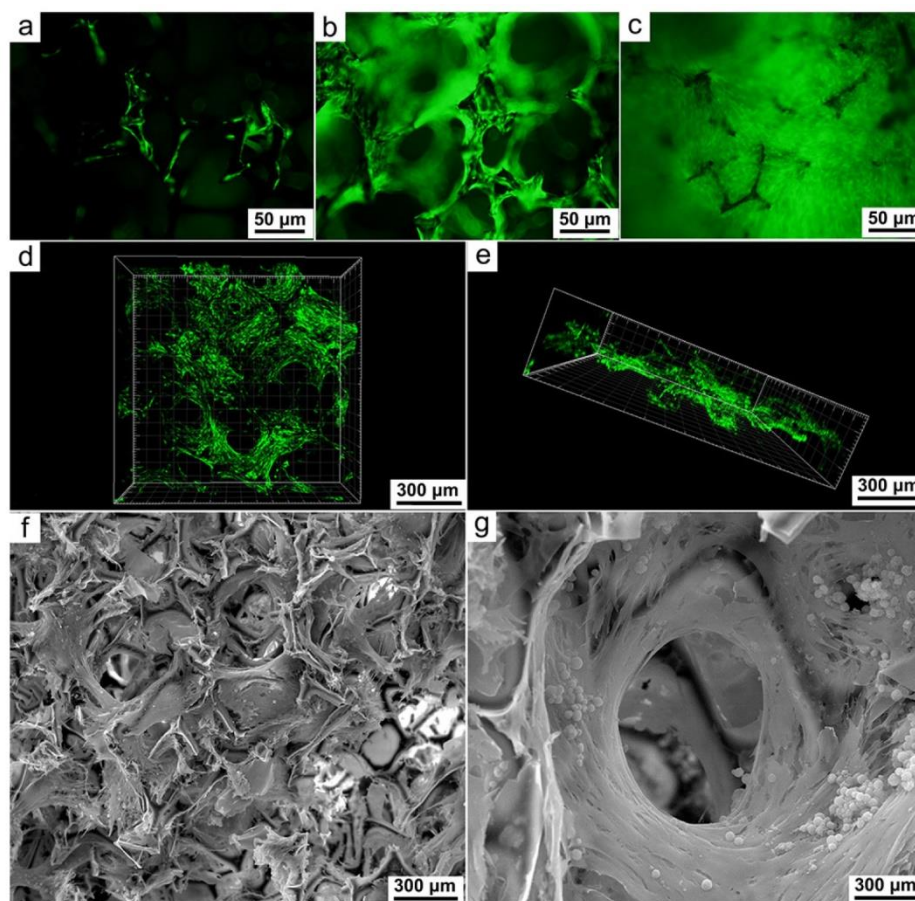


Figure 3. Fluorescence microscopic images showing the proliferation of stem cells in one day (a), three days (b) and seven days (c) after seeding onto the framework; Confocal imaging and 3D reconstruction indicating the extensive cell proliferation around and inside the framework at Day 7 (d, e); SEM images acquired at a depth of 1.5 mm to the surface (f), a thick layer of robustly proliferated cells can be seen enveloping the frame of the pore (g). The microchannel is clearly visible at the center of the pore and surrounded but otherwise unhindered by the proliferated cells.

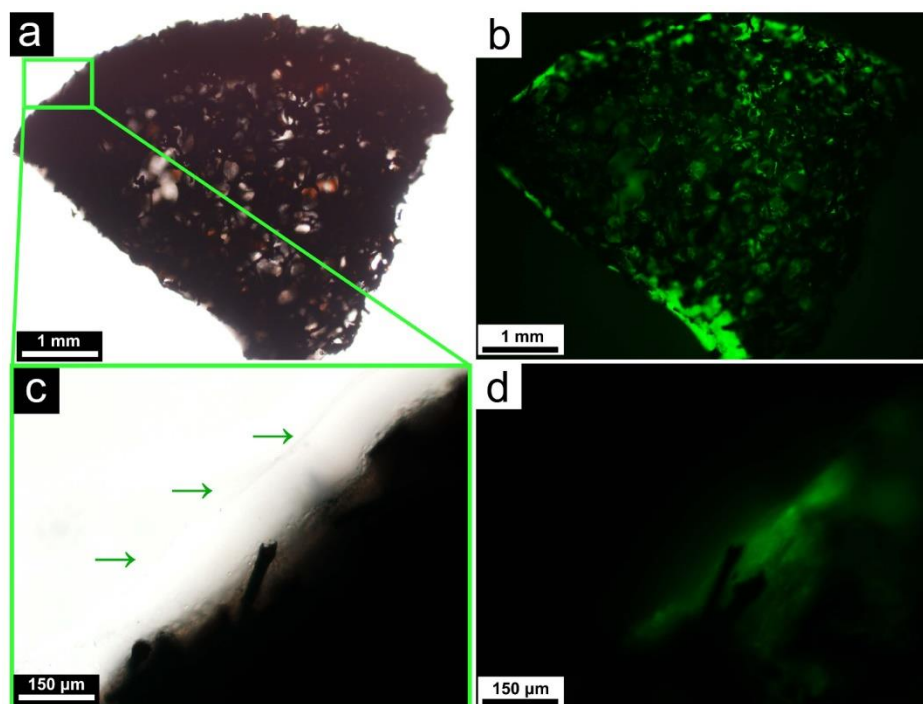


Figure 4. Light microscopic (a) and fluorescent microscopic (b) images of the matrigel-coated framework, demonstrating the continued viability of the cells after the coating; A close-up of the matrigel layer at the surface of the framework, as indicated by the green arrows. Both the light microscopic (c) and fluorescent microscopic (d) images are shown.

Neovasculature formation could also be clearly observed around the implanted area, which was indicated by the corresponding shadows cast in the fluorescent field of view (Figure 5c). The beneficial effect of the matrigel cover on the viability of the implanted cells was demonstrated by a control experiment in which a matrigel-free framework was used for implantation (Figure 5e). As a consequence, the fluorescence intensity around the implanted area was on average 61% lower compared to when a matrigel-covered framework was employed (Figure 5f). In addition, the effect of the implanted framework on heart functions was tested on rats with myocardial infarction using echocardiogram. Compared to the control that did not receive any implant, rats with myocardial infarction that were implanted with the framework showed a significant improvement in several aspects of cardiac functions, including stroke volume (fold-change = 1.63, $P < 0.05$), ejection fraction (fold-change = 1.32, $P < 0.05$) and fraction shortening (fold-change = 1.49, $P < 0.05$) (Figure 5g-l). These results indicated that the composite framework that we developed could indeed effectively promote heart tissue regeneration and considerably improve the performance of the infarct heart in rat models.

Discussion

To the best of our knowledge, the study described herein constitutes the first example of using an iron-oxide-based framework for tissue engineering. As an inorganic substance, iron oxide offers natural and highly tailorable porosity, excellent malleability and biodegradability. These features are some of the

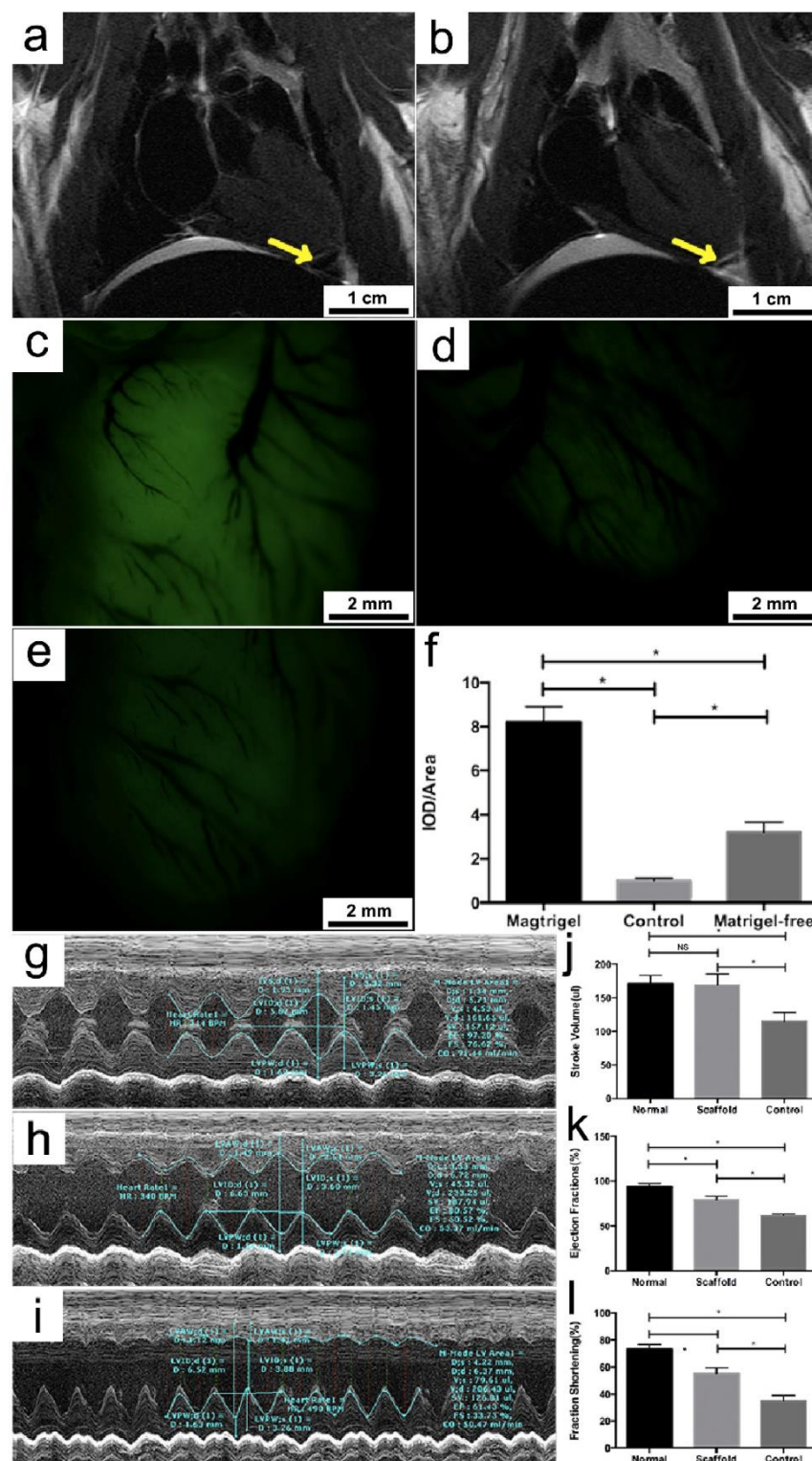


Figure 5. MRI scans showing the presence of the framework at the target area (indicated by the yellow arrow) immediately after the implantation (a) and the near-complete degradation of the framework in two months (b); fluorescence imaging of the target area on the heart where the framework was implanted: Significant growth of the implanted cells and regeneration of heart tissues can be seen two months after framework implantation (c) compared with the fluorescent background of the heart control with no framework implant (d); Matrigel-free framework showed low density of green fluorescence (e) compared to matrigel coating framework (f); Representative echocardiograms of a healthy rat (g), a rat with MI in which a framework was implanted (h), and a rat with MI as a control that did not receive any implant (i). Column charts comparing the stroke volume (j), ejection fraction (k) and fraction shortening (l) of the three above-mentioned rat models. Bars represent standard error of mean. NS indicates no statistical significance. * $P < 0.05$.

highly sought-after traits for tissue regrowth and implantation. Previously, the incorporation of inorganic materials in frameworks was almost entirely limited to various ceramics, hydroxyapatite (HA) or bioactive glasses, all of which are almost exclusively used in the regeneration of bone tissues [26, 27]. In contrast, no other type of inorganic framework or application of such framework in heart tissue engineering has been reported. The preparation of the iron oxide framework involved growing prussian blue nanotubes on a PU sponge via controlled hydrolysis of $K_4[Fe(CN)_6]$ and then submitting them to pyrolysis. This fabrication method exploits the high tailorability of the prussian blue template and is easily scalable at low cost [28]. In contrast, the size, shape and microscopic architecture of frameworks constructed from natural bioorganic materials are often restricted by the intrinsic mechanical and biological properties of the donor tissues or organs [29]. The generated iron oxide framework is characterized by its ultralight and porous architecture, which makes it particularly applicable to tissue regeneration and surgical implantation.

The availability of an interconnected porous architecture inside the framework plays a vital role in many essential functions, including nutrient transfer and 3D cell migration [13, 29], particularly for heart tissue grafting and vascularization [30]. To facilitate cell invasion into the interior framework, a careful calibration of the pore size has been conducted. The average pore size of a heart tissue framework needs to start in the vicinity of a few tens to hundreds of microns to accommodate myocardial and endothelial cells, with average sizes of 10 – 100 μm and 8 – 12 μm , respectively [31, 32]. When only surface neovascularization is concerned, the optimal pore size can be quite small [33]. But it is generally agreed that significantly larger pores between 100 and 500 μm are needed for the generation of extensive 3D vasculature networks, and this networks are thought to greatly increase the thickness and amount of tissues available for grafting [34]. For instance, an assessment of vessel invasion efficiency for various types of PEG-based hydrogels yielded the finding that pores with an average size of 100 – 150 μm resulted in considerably more extensive vessel generation inside the framework and a greater invasion area compared to the framework with pore sizes between 25 – 50 μm [35]. In this study, the results of SEM and fluorescent imaging demonstrated that the choice of iron oxide as the framework core material could conveniently lead to an average pore size around 200 μm , which promoted an extensive cell proliferation within a period of 4-7 days following the seeding. Moreover,

the large pores allowed the microchannels to remain generally unhindered, which would be beneficial for vascularization at the interior of the tissue framework. It should be emphasized that the porous network of our framework was also characterized by its high extent of interconnection. It has been reported that hydrogel-based frameworks with greater pore interconnectivity could exhibit twice as much invasion of proliferated cells inside the core compared to the ones with a similar distribution of pore size but fewer interconnections [36]. Consistent with these results, we found unambiguous evidence of cell ingrowth at a depth of 1.5 mm to the surface of the framework. The oxygen and nutrients that sustained the living cells at the depth of 1.5 mm should be facilitated by the porous structure instead of simple diffusion. This was supported by the finding that growth of tumor cells was limited to a maximum range of approximately 0.4 mm in the absence of blood vessel formation [37]. Taken together, the high porosity and interconnectivity of our framework promoted neovascularization and concomitantly allowed the cells to penetrate deeper as a result of better oxygen and nutrient transport.

In addition to the iron oxide core, we applied two additional layers of natural polymers that respectively comprised gelatin and matrigel. As thoroughly investigated in many other tissue engineering (TE) studies, gelatin displays excellent biocompatibility for enhancing cell adhesion and viability [38]. Indeed, the application of a gelatin-based intermediary layer exerted a potent surface-refining effect on the iron oxide framework that was initially not very conducive to cell adhesion. Importantly, the SEM imaging indicated that the gelatin layer did not significantly alter the porosity characteristics of the framework core, as the average pore size and the degree of interconnectivity remained roughly unchanged after the gelatin application. In addition, the matrigel-comprised outer cover was introduced not only for the purpose of improving the mechanical toughness of the framework and further increasing its biocompatibility with the infract region, but also for additional reasons with practical ramifications in surgery. First, the matrigel served as a protective layer against the external environment, particularly against potential sources of physical damage such as improper handling during surgery. Second, bathing the framework successively in increasingly concentrated matrigel solutions helped completely expel air bubbles from its porous interior. Since air trapped inside the pores is detrimental to both cell hydration and framework sterilization, matrigel envelopment of the framework could improve overall cell viability

and contribute to the robust spreading of graft tissues after implantation. Indeed, the use of a control framework lacking matrigel protection led to a substantial decrease in the number and density of viable myocardial cells, as indicated by fluorescence measurement, after *in vitro* incubation and surgical implantation. It should also be pointed out that compared to synthetic organic materials such as polylactic acid and polyglycolic acid, the gelatin and matrigel layers could provide more protein loci that facilitate cellular adhesion and migration [29].

A significant advantage of our study design was that the porous structure of our composite frameworks had the ability to sustain three-dimensional cell proliferation *in vivo* and *in vitro*. Moreover, the implantation experiments enabled us to directly monitor the biodegradability of our framework, a trait that is medically important but generally cannot be accurately evaluated via *in vitro* assays. In fact, disc-shaped PLGA frameworks that were implanted subdermally on rats were found to degrade faster than when subjected to *in vitro* degradation conditions [39]. In this study, the MRI scan suggested a near-complete degradation of the framework within two months. It should be noted that the moderate degradation rate of our composite framework allowed sufficient time for the integration of graft tissues and vasculature. Balancing degradation with porosity is a major technical concern in framework fabrication, as the high surface area of a porous framework, which is needed for cell proliferation, often results in its premature absorption after implantation [40]. The presence of multiple functional layers and the chemical nature of iron oxide played important roles in delaying the degradation of our framework *in vivo*.

After implantation, the mechanical force of heart contraction would cause the iron oxide core of the framework to disintegrate into particles, which would be phagocytized by macrophages and subsequently metabolized into soluble iron ions. The iron species could be stored in the form of ferritin or hemosiderin, or alternatively, released into the circulatory system and transported back to the marrow. The metabolism of iron derived from iron oxide nanoparticles has previously been investigated using Fe-labeled ferumoxytol [41]. It was found that iron was overwhelmingly retained, while organic components such as the carbohydrate coating were excreted [42, 43]. Due to the crucial role of iron in maintaining the viability of red blood cells, intravenous administration of iron-containing agents has been applied with success to the treatment of various anemia-related symptoms. For example, Garcia-Erce et al reported that intravenous injection of iron

sucrose significantly improved the hemoglobin levels and reduced the occurrence of anemia in patients undergoing knee replacement surgery [44]. Similar positive effects were also observed in a clinical study conducted by Toblli and co-workers, where substantially better cardiac and renal function parameters were associated with increased blood iron availability [45]. Furthermore, iron supplementation was also demonstrated to be beneficial for infarct reduction and left ventricular remodeling in patients with acute ST-elevation myocardial infarction [46]. Although the exact mechanism was unclear, the positive effect of iron was thought to be associated to its potential roles in stimulating the generation of mitochondrial adenosine triphosphate and/or eliciting anti-inflammatory response in macrophages that accelerated myocardial repair [47, 48]. These results suggested that the choice of iron oxide as the building material of the framework could potentially improve post-operative recovery of cardiac function in patients with myocardial infarction.

In summary, we have developed implantable and biodegradable macroporous framework consisting of an iron oxide core covered by a gelatin mid-layer and a matrigel outer layer. The framework was observed to possess a highly interconnected, porous architecture, high surface area ($\sim 85 \text{ m}^2/\text{g}$) with an average pore size of $200 \text{ }\mu\text{m}$ suitable for 3D tissue growth and vascularization. The seeded rat mesenchymal stem cells, sandwiched between the gelatin and the matrigel layers, demonstrated effective adhesion along the framework trabeculae and significant invasion into its porous interior within 4 to 7 days. Heart implantation experiments performed on healthy and infarct rats generated sufficient evidence for the framework's excellent biodegradability and effectiveness in promoting heart tissue regeneration *in vivo*. This work showcased a new approach using functional multilayer macroporous frameworks to effectively regenerate heart tissue *in vivo* and restore lost cardiac functions.

Abbreviations

ECM: extracellular matrix; MI: myocardial infarction; PGS: polymers poly(glycerol sebacate); PLGA: poly(lactide-co-glycolide); PEG: poly(ethylene glycol); PLGA: poly(lactic-co-glycolic acid; PU: polyurethane; SEM: scanning electron microscope; MRI: magnetic resonance imaging; HA: hydroxyapatite; TE: tissue engineering (TE); FESEM: The field emission scanning electron microscopy; PB: Prussian blue; PU: Polyurethane; PPI: pore sizes per linear inch; HCL: hydrochloric acid; DMEM: Dulbecco's Modified Eagle's medium; FBS: fetal

bovine serum; RR: respiration rate; LAD: left anterior descending artery.

Acknowledgement

This work was supported by Shanghai Sailing Program (grant number 17YF1402100); Shanghai Science and Technology Committee (grant number 14DZ1940902); Zhongshan Hospital Key Staffs Program (grant number 2015ZSYXGG05); and the NFSC (grant number 81501440, 81601663, 21322311, 21473038).

Competing Interests

The authors have declared that no competing interest exists.

References

- Ruvinov E, Cohen S. Alginate biomaterial for the treatment of myocardial infarction: Progress, translational strategies, and clinical outlook: From ocean algae to patient bedside. *Adv Drug Deliv Rev.* 2016;96:54-76.
- Zhang M, Methot D, Poppa V, et al. Cardiomyocyte grafting for cardiac repair: graft cell death and anti-death strategies. *J Mol Cell Cardiol.* 2001;33(5):907-21.
- Jawad H, Lyon AR, Harding SE, et al. Myocardial tissue engineering. *Br Med Bull.* 2008;87:31-47.
- Sui R, Liao X, Zhou X, et al. The current status of engineering myocardial tissue. *Stem Cell Rev.* 2011;7(1):172-80.
- Dvir T, Kedem A, Ruvinov E, et al. Prevascularization of cardiac patch on the omentum improves its therapeutic outcome. *Proc Natl Acad Sci USA.* 2009;106(35):14990-5.
- Davis ME, Hsieh PC, Grodzinsky AJ, et al. Custom design of the cardiac microenvironment with biomaterials. *Circ Res.* 2005;97(1):8-15.
- Glowacki J, Mizuno S. Collagen scaffolds for tissue engineering. *Biopolymers.* 2008;89(5):338-44.
- Cen L, Liu W, Cui L, et al. Collagen tissue engineering: development of novel biomaterials and applications. *Pediatr Res.* 2008;63(5):492-6.
- Kang HW, Tabata Y, Ikada Y. Fabrication of porous gelatin scaffolds for tissue engineering. *Biomaterials.* 1999;20(14):1339-44.
- Blan NR, Birla RK. Design and fabrication of heart muscle using scaffold-based tissue engineering. *J Biomed Mater Res A.* 2008;86(1):195-208.
- Gouveia RM, Castelletto V, Hamley IW, et al. New self-assembling multifunctional templates for the biofabrication and controlled self-release of cultured tissue. *Tissue Eng Part A.* 2015;21(11-12):1772-84.
- Sui R, Liao X, Zhou X, et al. The current status of engineering myocardial tissue. *Stem Cell Rev.* 2011;7(1):172-80.
- Lee KW, Wang Y. Elastomeric PGS scaffolds in arterial tissue engineering. *J Vis Exp.* 2011;(50).
- Kim SS, Sun PM, Jeon O, et al. Poly(lactide-co-glycolide)/hydroxyapatite composite scaffolds for bone tissue engineering. *Biomaterials.* 2006;27(8):1399-409.
- Burdick JA, Anseth KS. Photoencapsulation of osteoblasts in injectable RGD-modified PEG hydrogels for bone tissue engineering. *Biomaterials.* 2002;23(22):4315-23.
- Goktas M, Cinar G, Orujalipoor I, et al. Self-assembled peptide amphiphile nanofibers and peg composite hydrogels as tunable ECM mimetic microenvironment. *Biomacromolecules.* 2015;16(4):1247-58.
- Leong NL, Kabir N, Arshi A, et al. Evaluation of polycaprolactone scaffold with basic fibroblast growth factor and fibroblasts in an athymic rat model for anterior cruciate ligament reconstruction. *Tissue Eng Part A.* 2015;21(11-12):1859-68.
- Li M, Mondrinos MJ, Chen X, et al. Co-electrospun poly(lactide-co-glycolide), gelatin, and elastin blends for tissue engineering scaffolds. *J Biomed Mater Res A.* 2006;79(4):963-73.
- Martins AM, Eng G, Caridade SG, et al. Electrically conductive chitosan/carbon scaffolds for cardiac tissue engineering. *Biomacromolecules.* 2014;15(2):635-43.
- Qiao L, Swihart MT. Solution-Phase Synthesis of Transition Metal Oxide Nanocrystals: Morphologies, Formulae, and Mechanisms. *Adv Colloid Interfac.*
- Kong B, Tang J, Zhang Y, et al. Branched artificial nanofinger arrays by macroporous interfacial atomic rearrangement. *J Am Chem Soc.* 2015;137(12):4260-6.
- Kong B, Tang J, Selomulya C, et al. Oriented macroporous nanopillars as versatile plasmon-enhanced interfaces. *J Am Chem Soc.* 2014;136(19):6822-5.
- Kong B, Tang J, Zhang Y, et al. Incorporation of well-dispersed sub-5-nm graphitic pencil nanodots into ordered macroporous frameworks. *Nat Chem.* 2016;8(2):171-8.
- Kong B, Tang J, Wu Z, et al. Ultralight macroporous magnetic frameworks by interfacial assembly of Prussian blue nanocubes. *Angew Chem Int Ed Engl.* 2014;53(11):2888-92.
- Kempner P J, Greasley S, Parker K A, et al. Theranostic Mesoporous Silica Nanoparticles Biodegrade after Pro-Survival Drug Delivery and Ultrasound/Magnetic Resonance Imaging of Stem Cells. *Theranostics.* 2015;5(6):631-42.
- Fiorilli S, Bairo F, Cauda V, et al. Electrophoretic deposition of macroporous bioactive glass on glass-ceramic foam scaffolds for bone tissue engineering. *J Mater Sci Mater Med.* 2015;26(1):5346.
- Quinlan E, Lopez-Noriega A, Thompson E, et al. Development of collagen-hydroxyapatite scaffolds incorporating PLGA and alginate microparticles for the controlled delivery of rhBMP-2 for bone tissue engineering. *J Control Release.* 2015;198:71-9.
- Kong B, Selomulya C, Zheng G, et al. New faces of porous Prussian blue: interfacial assembly of integrated hetero-structures for sensing applications. *Chem Soc Rev.* 2015;44(22):7997-8018.
- Sabapathy V, Hurakadli M, Rana D, et al. Decellularized Amniotic Membrane Scaffold Compared to Synthetic PLGA and Hybrid Scaffolds Exhibit Superlative Biomechanical Properties for Tissue Engineering Applications. *J Biomater Tissue Eng.* 2016;6(7):549-562.
- Walthers CM, Nazemi AK, Patel SL, et al. The effect of scaffold macroporosity on angiogenesis and cell survival in tissue-engineered smooth muscle. *Biomaterials.* 2014;35(19):5129-37.
- Davis ME, Hsieh PC, Grodzinsky AJ, et al. Custom design of the cardiac microenvironment with biomaterials. *Circ Res.* 2005;97(1):8-15.
- Boffito M, Bernardi E, Sartori S, et al. A mechanical characterization of polymer scaffolds and films at the macroscale and nanoscale. *J Biomed Mater Res A.* 2015;103(1):162-9.
- Brauker JH, Carr-Brendel VE, Martinson LA, et al. Neovascularization of synthetic membranes directed by membrane microarchitecture. *J Biomed Mater Res.* 1995;29(12):1517-24.
- Ikada Y. Challenges in tissue engineering. *J R Soc Interface.* 2006;3(10):589-601.
- Chiu YC, Cheng MH, Engel H, et al. The role of pore size on vascularization and tissue remodeling in PEG hydrogels. *Biomaterials.* 2011;32(26):6045-51.
- Somo SI, Akar B, Bayrak ES, et al. Pore Interconnectivity Influences Growth Factor-Mediated Vascularization in Sphere-Templated Hydrogels. *Tissue Eng Part C Methods.* 2015;21(8):773-85.
- Roskoski RJ. Vascular endothelial growth factor (VEGF) signaling in tumor progression. *Crit Rev Oncol Hematol.* 2007;62(3):179-213.
- Shi C, Yuan W, Khan M, et al. Hydrophilic PCU scaffolds prepared by grafting PEGMA and immobilizing gelatin to enhance cell adhesion and proliferation. *Mater Sci Eng C Mater Biol Appl.* 2015;50:201-9.
- Sung HJ, Meredith C, Johnson C, et al. The effect of scaffold degradation rate on three-dimensional cell growth and angiogenesis. *Biomaterials.* 2004;25(26):5735-42.
- Hollister SJ. Porous scaffold design for tissue engineering. *Nat. Mater.* 2005;4(7):518-24.
- Usman A, Sadat U, Patterson AJ, et al. Use of ultrasmall superparamagnetic iron oxide particles for imaging carotid atherosclerosis. *Nanomedicine (Lond).* 2015.
- Neuwelt EA, Varallyay CG, Manninger S, et al. The potential of ferumoxylol nanoparticle magnetic resonance imaging, perfusion, and angiography in central nervous system malignancy: a pilot study. *Neurosurgery.* 2007;60(4):601-11, 611-2.
- MacDougall IC, Strauss WE, McLaughlin J, et al. A randomized comparison of ferumoxylol and iron sucrose for treating iron deficiency anemia in patients with CKD. *Clin J Am Soc Nephrol.* 2014;9(4):705-12.
- Garcia-Erce JA, Cuenca J, Martinez F, et al. Perioperative intravenous iron preserves iron stores and may hasten the recovery from post-operative anaemia after knee replacement surgery. *Transfus Med.* 2006;16(5):335-41.
- Tobli JE, Di Gennaro F, Rivas C. Changes in Echocardiographic Parameters in Iron Deficiency Patients with Heart Failure and Chronic Kidney Disease Treated with Intravenous Iron. *Heart Lung Circ.* 2015;24(7):686-95.
- Florian A, Ludwig A, Rosch S, et al. Positive effect of intravenous iron-oxide administration on left ventricular remodelling in patients with acute ST-elevation myocardial infarction - a cardiovascular magnetic resonance (CMR) study. *Int J Cardiol.* 2014;173(2):184-9.
- Lill R, Srinivasan V, Muhlenhoff U. The role of mitochondria in cytosolic-nuclear iron-sulfur protein biogenesis and in cellular iron regulation. *Curr Opin Microbiol.* 2014;22:111-9.
- Kai Z, Wu M, Hao L, et al. Nanoparticle-enhanced generation of gene-transfected mesenchymal stem cells for in vivo cardiac repair. *Biomaterials.* 2015;74:188-199.